Dimerization of the *Escherichia coli* Biotin Repressor: Corepressor Function in Protein Assembly[†]

Edward Eisenstein[‡] and Dorothy Beckett*[,§]

Center for Advanced Research in Biotechnology, University of Maryland Biotechnology Institute, National Institute of Standards and Technology, 9600 Gudelsky Drive, Rockville, Maryland 20850, Department of Chemistry and Biochemistry, University of Maryland Baltimore County, Baltimore, Maryland 21045, and Department of Chemistry and Biochemistry, College of Life Sciences, University of Maryland, College Park, Maryland 20472-2021

Received June 1, 1999; Revised Manuscript Received July 26, 1999

ABSTRACT: The repressor of biotin biosynthesis binds to the biotin operator sequence to repress transcription initiation at the biotin biosynthetic operon. Site-specific binding of BirA to the biotin operator is allosterically regulated by binding of the small molecule, biotinyl-5′-adenylate (bio-5′-AMP). The operator is a 40 base pair imperfect inverted palindrome and two holorepressor monomers bind cooperatively to the two operator half-sites. Results of previous detailed analyses of binding of holoBirA to *bioO* indicate that site-specific DNA binding and protein dimerization are obligatorily linked in the system. In the present work equilibrium sedimentation measurements have been used to examine the assembly properties of the aporepressor and its complexes with small ligands biotin and bio-5′-AMP. Results of these measurements indicate that while the free protein and the biotin complex exhibit no tendency to self-associate, the adenylate-bound protein assembles into dimers with an equilibrium constant of 11 μM. The results suggest that one mechanism by which the adenylate promotes binding of BirA to the biotin operator is by promoting repressor dimerization.

The repressor of biotin biosynthesis, BirA, binds site-specifically to the biotin operator sequence, *bioO*, to repress transcription initiation at the biotin biosynthetic operon (Figure 1a) (*1*). The repressor also functions as a biotin holoenzyme ligase by catalyzing linkage of biotin to the biotin carboxyl carrier protein (BCCP) of acetyl-CoA carboxylase (*1, 2*). This covalent linkage reaction occurs in two steps involving initial enzyme-catalyzed synthesis of the activated intermediate, biotinyl-5′-AMP, from substrates biotin and ATP (Figure 1a, step i), followed by transfer of the activated biotin to the ϵ-amino group of a unique lysine residue on BCCP (Figure 1a, step ii) (*3*). In this system the adenylate serves two functions: it is the activated intermediate in the biotin ligation reaction and the positive allosteric effector for site-specific DNA binding. Only the adenylate-bound form of BirA has been shown to bind tightly to *bioO* (Figure 1a, step iii) (*4*, *5*).

A three-dimensional structure of the unliganded or apo-biotin repressor has been obtained from X-ray crystallographic studies (*6*). The 35.3 kDa monomer is folded into three domains, the N-terminal, central, and C-terminal domains. The N-terminal domain, which adopts a "winged helix−turn−helix" fold, contacts the DNA in the holoBirA·*bioO* complex. The central domain contains the active site for adenylate synthesis and biotin transfer to BCCP. Since, however, adenylate binding is required for site-specific binding to *bioO*, the central domain is also required for high-affinity DNA binding. The function of the C-terminal domain has not yet been determined. As no evidence for the existence of other than crystal contacts between adjacent proteins is provided in the structure, the aporepressor is assumed to be monomeric.

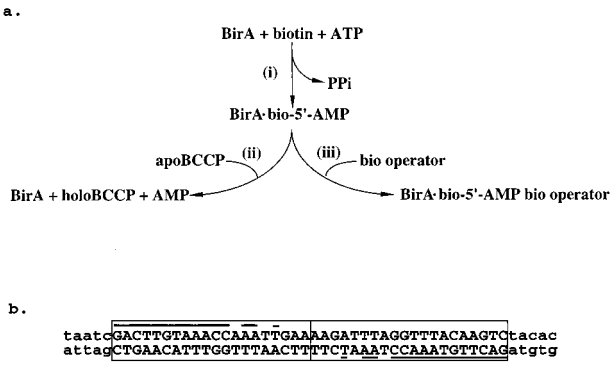

FIGURE 1: (a) Schematic representation of the *Escherichia coli* biotin regulatory system. The biotin repressor, BirA, (i) catalyzes synthesis of biotinyl-5′-AMP from substrates biotin and ATP, (ii) catalyzes transfer of biotin from the adenylate to the biotin carboxyl carrier protein (BCCP) subunit of acetyl-CoA carboxylase, and (iii) binds site-specifically to the biotin operator (*bioO*) to repress transcription initiation at the biotin biosynthetic operon. Biotinyl-5′-AMP is both the activated intermediate in biotin transfer and the allosteric effector in binding of BirA to *bioO*. (b) Sequence of the biotin operator. The 40-bp boxed sequence represents the operator. Underlined regions are conserved in the two 20-bp half-sites of the operator sequence (*7*). The five-base-pair termini are identical to the flanking sequences found in the biotin operon.

[†] Supported in part by NIH Grants GM46511 to D.B. and RR08937 to E.E.

* To whom correspondence should be addressed: e-mail dorothy_BECKETT@umail.umd.edu; phone 301-405-1812; fax 301-314-9121.

[‡] National Institute of Science and Technology and University of Maryland Baltimore County.

[§] College of Life Sciences, University of Maryland.

10.1021/bi991241q CCC: $18.00
Published on Web 09/15/1999

The biotin operator sequence is a 40 base pair imperfect inverted palindrome (Figure 1b) and two holoBirA monomers bind cooperatively to the two operator half-sites (*7*, *5*). Although the cooperative free energy for the binding process was originally estimated to be approximately −2 kcal/mol, results of more recent experiments involving measurements of binding of holoBirA to mutated operator sequences indicate a more favorable cooperative free energy on the order of −6.0 kcal/mol (*8*). The structural basis for cooperative binding of holoBirA to *bioO* may involve elements on the DNA or it may reflect direct interaction between protein monomers as they assemble onto the DNA. Results of structural probing of the holoBirA·*bioO* complex indicate that the DNA does undergo some distortion upon holoBirA binding and this distortion may contribute energetically to the observed cooperativity (*9*). We have previously examined the assembly properties of BirA using analytical gel-permeation chromatography. Results of these measurements indicated that no species larger than monomer is observed for apoBirA, BirA·biotin, or BirA-bio-5′-AMP (holoBirA) at protein concentrations as high as 1 μM (*5*). However, in studies of binding of holoBirA to biotin operator half-site mutants, no evidence supporting the existence of a measurable quantity of an intermediate species in which a monomer is bound to a wild-type *bioO* half-site was obtained at any level of saturation of the operator site (*8*). These latter results support a model in which site-specific binding to *bioO* and dimerization of holoBirA are highly coupled processes and prompted further examination of the assembly properties of BirA.

In this work we have used equilibrium sedimentation to examine the assembly properties of BirA at higher protein concentrations than those previously utilized. Results of these studies indicate that while apoBirA and the BirA·biotin complex show no tendency to aggregate at concentrations up to 100 μM, holoBirA undergoes association to dimer in the micromolar range of protein concentration. Global analysis of data obtained at multiple loading concentrations and rotor speeds are consistent with a simple monomer−dimer model for the association. These results in combination with previous studies of site-specific DNA binding in the system indicate that one means by which biotinyl-5′-AMP promotes assembly of the holoBirA−*bioO* complex is by promoting repressor dimerization.

MATERIALS AND METHODS

Chemicals and Biochemicals. All chemicals used in the preparation of buffers were at least reagent-grade. The D-biotin was purchased from Sigma. Bio-5′-AMP was synthesized by a modification of the method described in Lane et al. (*3*, *5*). BirA was purified according to the method described in Abbott and Beckett (*5*). The protein was estimated to be at least 95% pure as judged by results of SDS polyacrylamide gel electrophoresis. The BirA concentration was determined by using an extinction coefficient at 280 nm of 1.3 mL mg^{-1} cm^{-1} (*10*). An extinction coefficient for the protein at 295 nm was estimated from the ratio of the absorbance of the protein at this wavelength to its absorbance at 280 nm. An analytical molecular weight for BirA of 35 313 ± 8 was confirmed by matrix-assisted laser desorption ionization time-of-flight (MALDI-TOF) mass spectrometry.

Sedimentation Equilibrium Studies. Sedimentation equilibrium was used to determine the partial specific volume of unliganded BirA and the assembly properties of the protein. Experiments were carried out with a Beckman Optima XL-A analytical ultracentrifuge equipped with a four-hole, An-55 rotor. Standard 12 mm double-sector cells with charcoal-filled Epon centerpieces and quartz windows were used for all experiments. Protein concentration distributions were determined by using the absorption optical system of the instrument. All experiments were performed at 20 °C on samples that had been dialyzed extensively against the appropriate buffer. Sample volumes were typically 145 μL. The buffer compositions for all experiments are indicated in the Results section. For experiments performed in the presence of ligands, solutions were prepared by dissolving the ligand into the dialysate obtained from protein equilibration. Solvent densities were determined pycnometrically. Samples were run at multiple rotor speeds and multiple concentrations (*11*) and data were acquired as averages of 25 measurements of absorbance at each radial position, with nominal spacing of 0.001 cm between each position.

Preparation of Double-Stranded Oligonucleotides for DNA Binding Experiments. Single-stranded oligonucleotides used to prepare the double-stranded oligonucleotides used in gel mobility shift experiments were prepared by standard chemistry. The deprotected products were purified away from side products by electrophoresis on a 10% denaturing polyacrylamide gel (19:1 acrylamide:bisacrylamide). The oligonucleotides were stained with ethidium bromide and visualized under long-wavelength UV light. Gel fragments containing the oligonucleotides were excised and the DNA was electroeluted from the gel according to the method described in Maniatis et al. (*12*). The length of these oligonucleotides necessitated repetition of the gel purification in order to obtain homogeneity. The solution resulting from electroelution was concentrated by ethanol precipitation and the DNA was resuspended in 10 mM Tris-HCl and 0.1 mM EDTA, pH 8.0 at room temperature. The concentration of each oligonucleotide was determined by UV absorbance using an extinction coefficient at 260 nm of 0.02 mL mg^{-1} cm^{-1} (*12*).

The oligonucleotide corresponding to the top strand in Figure 1b was labeled at the 5′ terminus with ^{32}P using T4 polynucleotide kinase and [γ-^{32}P]ATP substrate. The double-stranded *bioO* oligonucleotide was prepared by combining the single-stranded unlabeled oligonucleotides at equimolar concentration (60 μM) with a trace amount of the ^{32}P-labeled top-strand oligonucleotide (final concentration approximately 9 nM) in 10 mM Tris-HCl, pH 8.0, and 0.1 mM EDTA. The sample was heated to 90 °C for 10 min and slow-cooled to room temperature. Complete hybridization of the oligonucleotides was confirmed by electrophoresing the sample on a 10% native polyacrylamide gel.

Gel Mobility Shift Experiments. Gel mobility shift experiments were performed following a modification of the methods described by Kim et al. (*13*). The buffer used in these reactions contained 10 mM Tris, pH 7.5 at 20 °C, 50 mM KCl, 2.5 mM $MgCl_2$, 1 mM $CaCl_2$, 3% (v/v) glycerol, and 0.1 mg/mL BSA. The electrophoresis buffer used contained 6.7 mM Tris, 1 mM EDTA, and 3.3 mM sodium acetate, pH 7.5 at 20 °C. Bio-5′-AMP was added to a final concentration of 10 μM. Each 25 μL reaction contained the

^{32}P-*bioO* oligonucleotide and BirA at total concentrations of 2×10^{-6} M and 4×10^{-6} M, respectively. Incubation was carried out at 20 °C for 30 min to allow the reactions to reach equilibrium. The samples were loaded onto a 10% (19:1 acrylamide:bisacrylamide) native acrylamide gel prepared in electrophoresis buffer that had been pre-electrophoresed at 100 V for 1 h with recirculation of the electrophoresis buffer provided by a peristaltic pump. The electrophoresis voltage was increased to 300 V, reactions were loaded directly onto the gel, and the voltage was decreased to 100 V for the duration of the 15 h run. The gel was dried and imaged by use of the Molecular Dynamics Phosphorimaging system.

Data Analysis. Sedimentation data were analyzed globally using a version of the NONLIN program (*14*, *15*) adapted for analysis of sedimentation equilibrium data (MacNONLIN). Equilibrium sedimentation data were initially analyzed by using a model for a single, homogeneous species according to (*16*)

$$c_r = \delta c + c_0 \exp[M(1 - \bar{v}\rho)\omega^2 (r^2 - r_0^2)/2\,RT] \quad (1)$$

where c_r is the total protein concentration at a given radial position, c_0 is the protein concentration at some reference position (in this case the first point in the data set), M is the molecular weight of the protein, $\bar{v}$ is the partial specific volume of the protein determined as described below, ρ is the solvent density, ω is the angular velocity of the rotor, r is the radial position in centimeters from the center of rotation, r_0 is the distance in centimeters from the center of rotation for the reference position (the first point in the data set), R is the gas constant, T is the absolute temperature, and δc is a correction term for a nonzero baseline. In nonlinear least-squares analysis with a single-species model, the data were fit to the reduced molecular weight, σ, defined by

$$\sigma = \frac{M(1 - \bar{v}\rho)\omega^2}{RT} \quad (2)$$

where the terms are as indicated above.

The molecular weight and partial specific volume of apoBirA were determined by performing sedimentation equilibrium experiments in buffers prepared with H_2O and D_2O (*18*). The primary data were analyzed in terms of eq 1 above and eq 3:

$$c_r = \delta c + c_0 \exp\left[kM\left(1 - \frac{\bar{v}}{k}\rho_{D_2O}\right)\omega^2 (r^2 - r_0^2)/2\,RT\right] \quad (3)$$

In this equation k is a proportionality constant for concomitant increase in molecular weight and decrease in partial specific volume that is observed in the heavier solvent D_2O as a result of deuterium exchange of all exchangeable hydrogens and ρ_{D_2O} is the density of the buffer prepared with D_2O. Based on a buffer composition of 95% (v/v) D_2O, a value for k of 1.0147 was used. As described above, the data were analyzed to obtained the best-fit value of σ at a range of fixed values of $\bar{v}$. The molecular weight was then calculated from the reduced molecular weight by use of eq 2.

Equilibrium sedimentation data were also analyzed by use of models that included terms for monomer and higher order aggregates of the protein:

$$c_r = \delta c + \sum c_i(r) \quad (4)$$

where δc is the baseline correction term and $c_i(r)$ is the concentration of each species (monomer, dimer, etc.) as a function of radial position. Combining the relationship between the each species concentration and the monomer concentration and equilibrium constant governing assembly with eq 1 yields the following (*16*):

$$c_r = \delta c + \sum (c^i{}_{0_1} K_{a1 \leftrightarrows i} e^{i\sigma_i \xi}) \quad (5)$$

where $c^i{}_{0_1}$ is the monomer concentration at some reference position to the ith power (where i refers to the degree of association), $K_{a1 \leftrightarrows i}$ is the equilibrum association constant governing assembly monomer to i-mer, σ_i is the reduced buoyant molecular weight of the i-mer, and ξ is equivalent to $(r^2 - r_0^2)/2$, where r_0 is the reference position and r is the radial position. In the analysis the reduced buoyant molecular weight of an i-mer was assumed to be equivalent to the value for the monomer multiplied by the degree of association ($\sigma_i = i\sigma_1$). Data were analyzed with several stoichiometric models for the assembly process that are described in the Results section.

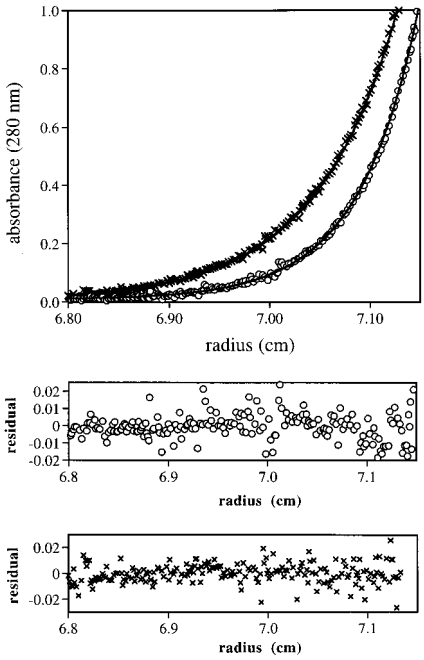

FIGURE 2: Concentration (in absorbance units) vs radial position profiles for apoBirA obtained in buffer prepared in (×) D_2O and (○) H_2O. Loading concentration (6 μM), rotor speed 24 000 rpm. Buffer composition was 10 mM Tris-HCl pH 7.50 at 20 °C, 50 mM KCl, and 2.5 mM $MgCl_2$. The solid lines were simulated by using the parameters obtained from global nonlinear least-squares analysis of data obtained at 24 000 and 26 000 rpm. The two lower panels illustrate the residuals of the fits for the two data sets.

RESULTS

Partial Specific Volume of ApoBirA. The method of Edelstein and Schachman (*17*) was utilized to determine the partial specific volume and molecular weight of BirA. The measurement involves simultaneous analysis of equilibrium sedimentation data obtained on the protein dissolved in buffer

Table 1: Results of Equilibrium Sedimentation Analysis of ApoBirA and the BirA·Biotin Complex

sample/model	loading concentrations[a] (μM)	rotor speeds (rpm)	molecular weight or equilibrium constant[b]	(var)$^{1/2}$ [c]
		ApoBirA		
single species	10, 40	24 000, 26 000	32 087 (31 605/32 406)	0.004
monomer−dimer[d]			$K_{2-1} = 1.6 \times 10^{-2}$ $(4 \times 10^{-3}/2 \times 10^{-1})$	0.004
		BirA·Biotin[f]		
single species	10, 40	24 000, 26 000	31 936 (31 455/32 418)	0.004
monomer−dimer			$K_{2-1} = 3 \times 10^{-3}$ $(1 \times 10^{-3}/7 \times 10^{-3})$	0.004

[a] Initial total protein monomer concentration in the cell. [b] Molecular weights (with 67% confidence limits) were calculated from the reduced molecular weights obtained from global nonlinear least-squares analysis of five equilibrium sedimentation data sets with a single-species model. The relationship of the reduced molecular weight (σ) to the molecular weight is provided in the data analysis section of Materials and Methods. [c] Square root of the variance of the fit. [d] The data were fit to a monomer−dimer association model. The equilibrium dissociation constant for the dimerization reacion, K_{2-1}, is given in molar units with the lower and upper confidence intervals in parentheses. The monomer molecular weight was fixed at the best fit value obtained for the single species fit. [e] In analysis of the data by the monomer−dimer assembly model, the monomer molecular weight was fixed at the value obtained by use of the single-species model. [f] In all cases the biotin concentration was at least 1.5 times the total protein monomer concentration.

prepared in H_2O and D_2O. Results of the measurements are shown in Figure 2. Global analysis of the data obtained in the two buffers at two different rotor speeds yielded a value of the molecular weight of 36 400 (35 400/37 700) using partial specific volume of 0.755 mL/g. The resolved value of the molecular weight is in good agreement with that determined by MALDI-TOF mass spectrometry (see Materials and Methods).The value of the partial specific volume, although higher than the value of 0.73 mL/g calculated on the basis of the amino acid composition (*18*, *19*), is within the range previously found for proteins (*20*).

Assembly Properties of ApoBirA, BirA·Biotin, and Holo-BirA. Sedimentation equilibrium measurements were used to determine the assembly properties of apoBirA and its complexes with biotin and biotinyl-5′-AMP. Biotin is a substrate for the synthesis of biotinyl-5′-AMP catalyzed by BirA. Bio-5′-AMP is both the active intermediate in transfer of biotin to the biotin carboxyl carrier protein (BCCP) subunit of the acetyl-CoA carboxylase and the positive allosteric effector for DNA binding. Two holoBirA bind cooperatively to the two half-sites of the biotin operator. There is, thus, a thermodynamic interaction between the two protein monomers in the assembly of the holoBirA·*bioO* complex. The sedimentation experiments were performed to investigate the possible existence of a physical interaction between the protein monomers in the absence of DNA and to examine the role of small ligands in the assembly reaction.

Results of sedimentation equilibrium experiments performed on apoBirA are shown in Figure 3. These experiments were performed at two loading concentrations and three rotor speeds. The results of nonlinear least-squares analysis of the data are shown in Table 1. Global analysis of the data with a model that assumes a single species yielded a molecular weight for the protein that is within 10% of that expected for the protein monomer. The data were also analyzed with models in which the occurrence of an equilibrium between monomers and higher order oligomers of apoBirA was assumed. Models incorporating a dimeric or trimeric species in addition to the monomer were tested, and results of the analyses provided no evidence supporting the presence of any of these larger species at the concentrations employed for the measurements. For example, as shown in Table 1, although analysis of the data with a monomer−dimer model does yield a best-fit value for the equilibrium constant for the reaction in the millimolar range of concentration, this number has no significance for two reasons. First, the standard error in the best-fit parameter is very large. Second, the apoBirA monomer concentrations utilized for the measurements do not approach the millimolar range. Thus, over the concentration range employed the apoprotein is monomeric.

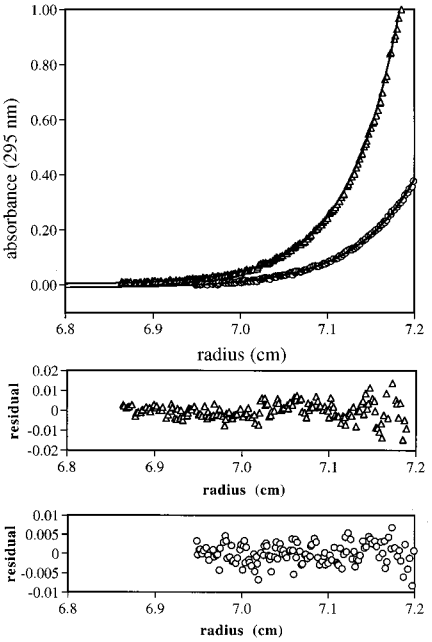

FIGURE 3: Concentration (in A_{295} units) vs radial position profiles for apoBirA obtained in buffer A (10 mM Tris-HCl, pH 7.50 at 20 °C, 200 mM KCl, and 2.5 mM $MgCl_2$). Loading concentrations (BirA monomer) and rotor speed: (○) 10 μM and 24 000 rpm; (△) 40 μM and 26 000 rpm. The solid line was simulated by using the parameters obtained from global analysis of five data sets obtained at these two loading concentrations and rotor speed ranging from 24 000 to 26 000 rpm with a single-species model. The two lower panels illustrate the residuals of the fits of the two data sets to the single-species model.

The BirA·biotin complex was also subjected to equilibrium sedimentation. Results of previous studies indicate that the equilibrium dissociation constant governing biotin binding to BirA is 4×10^{-8} M in buffer conditions identical to those used for the sedimentation measurements (*21*). The protein is, therefore, saturated with ligand in the centrifugation experiments. Concentration vs radial position profiles obtained in these measurements are shown in Figure 4. Analysis

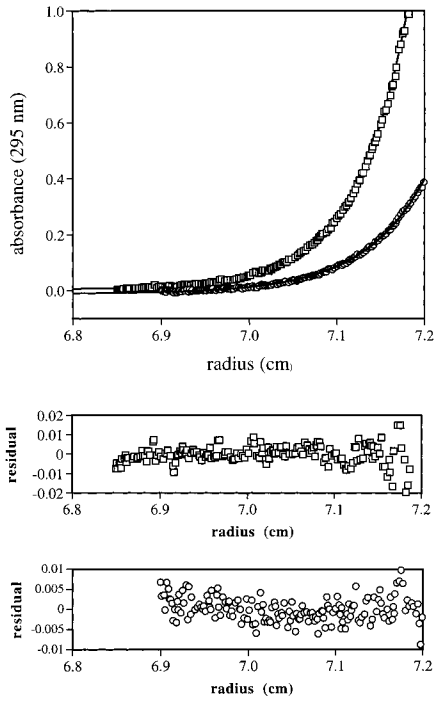

FIGURE 4: Concentration (in A_{295} units) vs radial position profiles for BirA·biotin obtained in buffer A. Loading concentrations and rotor speed: (○) 10 μM BirA, 15 μM biotin, and 24 000 rpm; (□) 40 μM, 60 μM biotin, and 26 000 rpm. The solid line was simulated by using the parameters obtained from global analysis of five data sets obtained at these two loading concentrations and rotor speed ranging from 24 000 to 26 000 rpm with a single-species model. The two lower panels illustrate the residuals of the fits of the two data sets to the single-species model.

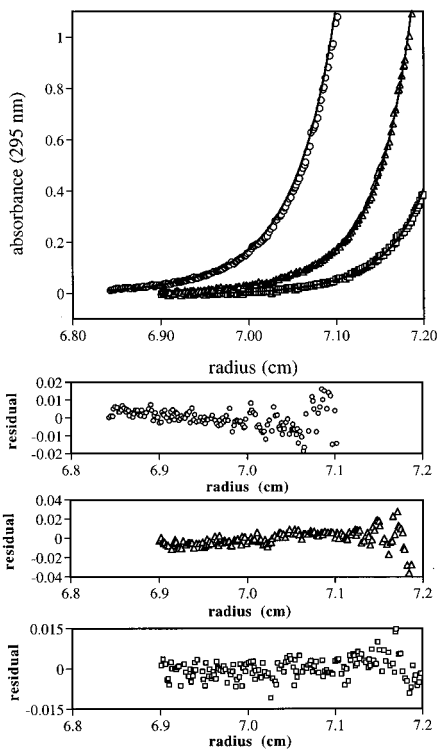

FIGURE 5: Concentration (A_{295} units) vs radial position profiles for BirA·bio-5′-AMP obtained in buffer A. Loading concentrations and rotor speeds: (□) 10 μM BirA, 20 μM bio-5′-AMP, and 24 000 rpm; (△) 40 μM BirA, 60 μM bio-5′-AMP, and 24 000 rpm; (○) 60 μM BirA, 180 μM bio-5′-AMP, and 22 000 rpm. The solid lines were simulated by using the parameters obtained from global analysis of seven data sets obtained at these three loading concentrations and rotor speeds ranging from 22 000 to 26 000 rpm with a monomer−dimer model for the assembly process. The three lower panels illustrate the residuals of the fits of the three data sets to the monomer−dimer model.

of the data with a single-species model indicates a molecular weight for the complex consistent with that of the monomer. As was found for apoBirA, analysis of the data with models for self-association of the complex (monomer−dimer, monomer−trimer) provide no evidence supporting the contribution of any oligomeric species to the species population at the protein concentrations employed (Table 1). The equilibrium dissociation constant for a monomer−dimer process obtained for the biotin-bound protein is 3 mM. Given that the highest protein concentrations observed in the sedimentation profiles are in the micromolar range of concentration, this resolved value for the dimerization constant has no significance.

Results of sedimentation equilibrium measurements performed on the BirA·bio-5′-AMP complex (holoBirA) are shown in Figure 5. These measurements were performed at three loading concentrations and three rotor speeds. The equilibrium dissociation constant governing binding of BirA to bio-5′-AMP has been measured and is approximately 4×10^{-11} M in buffer conditions identical to those used for the sedimentation measurements (*21*, *22*). Therefore, at the concentrations employed the protein is saturated with bio-5′-AMP. Global analysis of the data using a model that assumes a single species yields a molecular weight for holoBirA considerably higher than that expected of the monomeric complex (Table 2). This result is consistent with self-assembly of the holorepressor and the data were further analyzed with models that, in addition to the monomer, incorporate higher order species. A simple monomer−dimer model was initially tested. Comparison of the quality of the fit based on the values of the square root of the variance indicate that the data are better described by this simple model for association than by a single-species model (Table 2). The value for the monomer−dimer equilibrium constant obtained from the analysis is 11 μM. Models incorporating larger oligomeric species were also tested. As indicated in Table 2, no support for models involving direct assembly of the monomeric holoBirA into a trimeric or tetrameric species is provided by the analysis. This conclusion is based on the quality of the fits as judged by the large values of the square root of the variance (Table 2). The data were also analyzed with models that assumed, in addition to monomer and dimer, contributions of trimeric or tetrameric species to the association process. On the basis of comparison of the values of the square root of the variance of the fits with these two more complex models versus a simple monomer−dimer model, it is difficult to absolutely rule out the contribution of higher order species. In fact, the slightly nonrandom nature of the residuals of the fit of the data to a simple monomer−dimer model observed at the highest protein concentration (Figure 5) suggests the contribution of higher order oligomers to the species population. However, the best-fit values for the equilibrium dissociation constant governing the monomer−dimer equilibrium obtained from data analysis using these more complicated models confirm the 11 μM value obtained from analysis with a simple monomer−dimer model. Moreover, given the magnitudes of the equilibrium constants governing formation of the trimer or tetramer, even at the highest protein concentrations observed in the sedimentation

Table 2: Results of Analysis of Sedimentation Equilibrium Measurements of HoloBirA[a]

model	molecular weight	K_{n-1}[b]	(var)$^{1/2}$ [e]
single species	51 363 (50 027/53 082)[b]		0.009
monomer−dimer	(32 087)	1.1×10^{-5} (8.3×10^{-6}/1.3×10^{-5})	0.0067
monomer−trimer	(32 087)	2.8×10^{-5} (2.2×10^{-5}/3.5×10^{-5})	0.010
monomer−tetramer	(32 087)	3.5×10^{-5} (2.2×10^{-5}/5.0×10^{-5})	0.015
monomer−dimer−trimer	(32 087)	K_{2-1} 1.2×10^{-5} (1.1×10^{-5}/1.4×10^{-5}) K_{3-1} 7.5×10^{-5} (4.3×10^{-5}/1.6×10^{-4})	0.0066
monomer−dimer−tetramer	(32 087)	K_{2-1} 1.1×10^{-5} (1.0×10^{-5}, 1.2×10^{-5}) K_{4-1} 1.0×10^{-4} (3.0×10^{-5}, 8.0×10^{-4})	0.0066

[a] Parameters were obtained from global nonlinear least-squares analysis of seven data sets. The data were obtained at three loading concentrations (10, 40, and 60 μM) and rotor speeds ranging from 22 000 to 26 000 rpm. In all samples the bio-5′-AMP was present at a concentration at least 1.5 times greater than the total BirA monomer concentration. [b] K_{n-1} refers to the equilibrium dissociation constant governing the monomer−dimer, monomer−trimer, or monomer−tetramer assembly processes. The 67% confidence limits are provided in parentheses. [c] Square root of the variance of the fit. [d] The 67% confidence limits. [e] In analysis of the data with models that incorporate self-association, the monomer molecular weight was fixed at the value obtained from nonlinear least-squares analysis of equilibrium sedimentation experiments performed on apoBirA. See Table 1.

profiles, results of species concentration analysis indicates that trimer or tetramer constitute 4% and 1% of the total species population, respectively. Approximately 75% of the protein is dimeric at these same protein concentrations. Furthermore, as indicated below, it is the dimeric species that is relevant to site-specific binding of holoBirA to *bioO*.

Direct Evidence of the 2:1 Stoichiometry for the HoloBirA·bioO Complex. We have previously measured the stoichiometry of the holoBirA·*bioO* complex using the nitrocellulose filter binding assay and obtained a value of 2 holoBirA monomers/operator site (*5*). Analysis of the data obtained by this method is based on the assumption that both the protein and DNA fragment used for the measurements are fully active in binding. To confirm the stoichiometry by a method that does not rely on these same assumptions, we performed gel mobility shift experiments with mixtures of wild-type BirA (wtBirA) and a BirA derivative (dBirA). In this derivative the recognition sequence, VRRAS, for a cyclic AMP-dependent protein kinase and a hexahistidine sequence are fused to the amino and carboxy termini of BirA, respectively. This derivative has been demonstrated to behave identically to wild-type BirA at all levels measured including *bioO* binding (Streaker and Beckett, submitted for publication). In the gel mobility shift experiment a 50 base pair double-stranded oligonucleotide containing the 40 base pair operator site in the context of two 5 base pair flanking sequences identical to those that are found in the biotin operon region (Figure 1b) was incubated with either wtBirA, dBirA, or an equimolar mixture of wtBirA and dBirA. The allosteric effector, bio-5′-AMP, was present at saturating concentration in each sample. In all samples the molar ratio of protein monomer to DNA duplex is 2:1. As shown in Figure 6 only one type of protein·DNA complex is formed in the presence of either wtBirA or dBirA alone. Moreover, the two protein·DNA complexes exhibit distinct mobilities. However, when a mixture of the two proteins is combined with the oligonucleotide, three distinct bands are observed. Two of these are characterized by mobilities identical to those obtained for the complexes formed from the individual proteins. The third more intense band, which is characterized by a mobility intermediate between those observed for the single protein complexes, presumably arises from binding of a heterodimer of wtBirA and dBirA to the oligonucleotide. This result indicates that, as expected for a 2:1 stoichiometry, in the sample containing wtBirA and the derivative the protein is distributed among three complexes: two in which

FIGURE 6: Results of imaging electrophoretic mobility shift measurements of holoBirA·*bioO* complexes prepared by using a 50 base pair oligonucleotide containing the *bioO* sequence (Figure 1B) and (1) wild-type BirA, (2) a 1:1 mixture of wild type and the variant BirA (dBirA), and (3) variant BirA (dBirA). Buffer composition and concentrations are provided in Materials and Methods. The cartoon illustrates the expected distribution of the two types of BirA monomers given a holoBirA:*bioO* stoichiometry of 2:1.

a homodimer of each protein is bound to DNA and one in which a heterodimer is bound. A stoichiometry greater than 2:1 is expected to result in the appearance of a greater number of bands characterized by mobilities between those corresponding to the homodimeric complexes. Furthermore, as expected for a statistical distribution of the two types of protein monomers in the complexes, quantitation of the optical density in the three bands indicates that the intensity of central band corresponding to the heterodimer complex is 2-fold greater than that of the two bands corresponding to the homodimeric complexes.

DISCUSSION

ApoBirA and BirA·Biotin Are Monomeric. The assembly state of BirA and its small ligand complexes has been previously investigated by large- and small-zone analytical gel-permeation chromatography. Results of these measurements indicated that the free protein and its complexes with biotin and bio-5′-AMP are monomeric at concentrations as high as 1 μM (*5*). In this work the assembly studies have been extended to higher concentrations. Results of the sedimentation equilibrium studies indicate that the aporepressor and the BirA·biotin complex are both monomeric at the concentrations utilized for the measurements.

The Assembly Properties of HoloBirA. The complex of BirA with bio-5′-AMP undergoes a dimerization reaction in

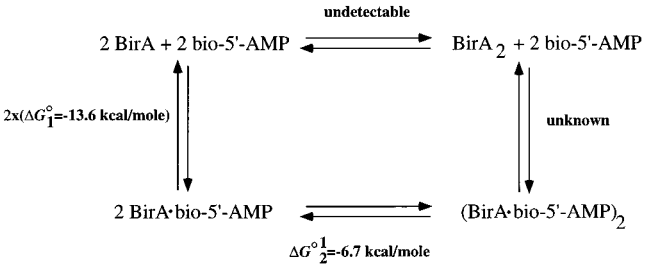

FIGURE 7: Thermodynamic cycle illustrating the linkage between BirA dimerization and binding of bio-5′-AMP. The standard Gibbs free energy for binding of bio-5′-AMP to the BirA monomer is $\triangle G°_1$, The standard Gibbs free energy governing dimerization of holoBirA is $\triangle G°^1_2$.

the micromolar range of protein concentration and the best-fit value for the equilibrium dimerization constant of holoBirA is 11 μM. This value for the dimerization constant is supported by results of analysis of the sedimentation data with a simple monomer−dimer model as well as more complex assembly models that incorporate trimeric or tetrameric holoBirA in addition to the monomer and dimer. Although the data do not rule out the existence of larger oligomers of holoBirA at higher protein concentrations (0.1−1.0 mM), these concentrations are far greater than the physiologically relevant concentration of approximately 20 nM (*23*, *24*). Furthermore, examination of the results of analysis of the data with models in which a dimeric species is not included clearly support the significance of the dimer in assembly of holoBirA. Moreover, as illustrated previously in stoichiometric titrations (*5*) and in this work in gel shift experiments performed with mixtures of wild-type BirA and a BirA derivative, it is the holoBirA dimer species that is relevant to site-specific binding of the biotin repressor to *bioO*.

Linkage of Dimerization and Bio-5′-AMP Binding. The results of the equilibrium sedimentation measurements indicate that the adenylated form of biotin, bio-5′-AMP, acts as an allosteric activator of assembly of the BirA dimer. Bio-5′-AMP is both the active intermediate in the enzymatic transfer of biotin to BCCP and the positive allosteric effector for site-specific binding of BirA to the biotin operator sequence. We have previously shown that two holoBirA monomers bind cooperatively to the two half-sites of the biotin operator sequence. The magnitude of cooperative free energy for the holoBirA−*bioO* interaction is on the order of −6 kcal/mol. This conclusion is based on the lack of observance of any species in which a holoBirA monomer is associated with a *bioO* half-site sequence, even in an operator mutant in which one wild-type half-site is replaced by "nonspecific" flanking sequences. These latter results highlight the obligatory coupling of dimerization and site-specific DNA binding in this system. The linkage between repressor dimerization and adenylate binding observed in this work provides a mechanism by which the corepressor promotes the site-specific binding of BirA to *bioO*.

A thermodynamic cycle illustrating the linkage between bio-5′-AMP binding and dimerization is shown in Figure 7. The Gibbs free energy for binding of bio-5′-AMP to the BirA monomer has been previously determined (*21*, *22*). The Gibbs free energy for dimerization of the liganded protein was calculated using the best-fit value of the equilibrium dimerization constant for this species. The current data provide no information about the energetics of dimerization of apoBirA and, on the basis of the best-fit value for a dimerization constant for the unliganded protein shown in Table 1, examination of the protein at concentrations as high as 0.3 M may be required to obtain reliable parameters for its assembly. The stability of the complex formed between the BirA monomer and bio-5′-AMP is very high and due to reciprocity the dimeric BirA·bio-5′-AMP complex is predicted to be more stable. We have qualitatively confirmed this prediction by comparing the rate of dissociation of the ligand from the monomer to that from a mixture of monomers and dimers. At protein concentrations at which, on the basis of the equilibrium dissociation constant reported in this work, a significant fraction of the protein is dimeric, the rate of release of the adenylate from BirA is immeasurably slow by the method employed (Xu and Beckett, unpublished results).

Corepressor That Drives Protein Assembly. The accumulated data indicate that bio-5′-AMP acts, in part, as a positive allosteric effector for site-specific DNA binding by driving dimerization of BirA. Although protein assembly has been shown to contribute significantly to the assembly of many transcriptional regulatory complexes, there are few examples in which a functional role of a small ligand in these protein−protein interactions has been directly demonstrated. Among these are the tyrosine repressor from *Escherichia coli* tyrosine and the *Synechococcus* metallothionein repressor (*25*, *26*). The former exhibits linkage of dimerization and hexamerization to ATP and tyrosine binding and the latter protein dimerizes in a metal-dependent reaction. In the eukaryotic nuclear receptors, including the 1,25-dihydroxyvitamin D_3 and 9-*cis*-retinoic acid receptors, evidence exists that regulatory ligands play roles in determining not only the homooligomeric state of the receptor but also the assembly of heterooligomers of more than one receptor type (*27*). This regulation of dimer binding partner has consequences for target site selection in site-specific DNA binding (*28*). In general, these effector-linked assembly processes provide an indirect means of regulating DNA target site occupancy, and ultimately transcriptional activity, via small ligand concentration.

Multifunctional Corepressor. Biotinyl-5′-AMP functions not only as the corepressor in the binding of BirA to *bioO* but also as the activated intermediate in transfer of biotin to acetyl-CoA carboxylase. This dual functionality renders it unique among the known small ligand modulators of site-specific DNA binding. The corepressor function of the adenylate may simply reflect its ability to promote the dimerization of BirA that is coupled to *bioO* binding. We hypothesize that the dimerization function of bio-5′-AMP was acquired relatively recently in the evolution of the protein. This hypothesis is based on the idea that evolution of the means to catalyze synthesis of the adenylate presumably preceded acquisition of the dimerization function. As demonstrated in studies of staphyloccocal nuclease, acquisition of dimerization function by a monomeric protein can be achieved with very few changes in amino acid sequence (*29*). The evolution of coupling between adenylate binding and dimerization is most likely more complex. Comparative studies of BirA and other members of the biotin holoenzyme synthetase enzyme family that do not function as repressors may provide some insight into the structural basis for

acquisition of this linkage in the protein.

Role for DNA in Biotin Repressor Dimerization. The equilibrium dissociation constant of 11 μM determined in this work for the dimerization of holoBirA indicates that the holoBirA dimer is only moderately stable. At the physiologically relevant nanomolar protein concentrations that are also relevant for specific binding to *bioO*, holoBirA is essentially 100% monomer (*23*, *24*). The observation that the final complex, at 10 nM protein concentration, consists of holoBirA dimer bound to *bioO* and that no monomer−DNA species is ever observed suggests that biotin repressor dimerization, in addition to being driven by binding of bio-5′-AMP, may also be a DNA-induced process. Results of more detailed equilibrium thermodynamic studies will reveal the magnitude of this linkage.

Site-specific DNA binding proteins range from those those that form stable oligomeric species that bind to DNA in a preassembled state to those that exhibit weak association, either homo- or heterotypic, and assemble on the DNA. It has been suggested in some cases that this latter behavior may be significant for lowering the kinetic barrier to the association of the protein with DNA (*30*). However, in the biotin regulatory system the weak dimerization of holoBirA may instead reflect the requirements of its second function in catalyzing posttranslational linkage of biotin to acetyl-CoA carboxylase which may require the monomeric holo-BirA species. In fact, results of preliminary studies of BirA mutants indicate that the same surface of the protein is utilized both for dimerization and for the interaction with the biotin carboxyl carrier protein subunit of acetyl-CoA carboxylase.

REFERENCES

1. Cronan, J. E., Jr. (1989) *Cell 58*, 427−429.
2. Barker, D. F., and Campbell, A. M. (1981) *J. Mol. Biol. 146*, 469−492.
3. Lane, M. D., Rominger, K. L., Young, D. L., and Lynen, F. (1964) *J. Biol. Chem. 239*, 2865−2871.
4. Prakash, O., and Eisenberg, M. A. (1979) *Proc. Natl. Acad. Sci. U.S.A. 76*, 5592−5595.
5. Abbott, J., and Beckett, D. (1993) *Biochemistry 32*, 9649−9656.
6. Wilson, K. S., Shewchuk, L. M., Brennan, R. G., Otsuka, A. J., and Matthews, B. W. (1992) *Proc. Natl. Acad. Sci. 89*, 9257−9261.
7. Otsuka, A. J., and Abelson, J. (1978) *Nature 276*, 689−693.
8. Streaker, E. D., and Beckett, D. (1998) *Biochemistry 37*, 3210−3219.
9. Streaker, E. D., and Beckett, D. (1998) *J. Mol. Biol. 278*, 787−800.
10. Gill, S. C., and von Hippel, P. H. (1989) *Anal. Biochem. 182*, 319−326.
11. Roark, D. E. (1976) *Biophys. Chem. 5*, 185−196.
12. Maniatis, T., Fritsch, E. F., and Sambrook, J. (1982) *Molecular Cloning, A Laboratory Manual*, Cold Spring Harbor Laboratory, Cold Spring Harbor, NY.
13. Kim, J., Zwieb, C., Wu, C., and Adhya, S. (1989) *Gene 85*, 15−23.
14. Johnson, M. L., Correia, J. J., Yphantis, D. A., and Halvorson, H. R. (1981) *Biophys. J. 36*, 575−588.
15. Johnson, M. L. and Frasier, S. G. (1989) *Methods Enzymol. 117*, 301.
16. Laue, T. M. (1995) *Methods Enzymol. 259*, 427−452.
17. Edelstein, S. J. and Schachman, H. K. (1967) *J. Biol. Chem. 242*, 306−311.
18. Durschlag, H. (1986) in *Thermodynamic Data for Biochemistry and Biotechnology* (Hinz, H. J., Ed.) p 45, Springer-Verlag, Berlin.
19. Howard, P. K., Shaw, J., and Otsuka, A. J. (1985) *Gene 35*, 321−331.
20. Fasman, G., Ed. (1976) *Handbook of Biochemistry and Molecular Biology*, 3rd ed., CRC Press, Cleveland, OH.
21. Xu, Y., Nenortas, E., and Beckett, D. (1995) *Biochemistry 34*, 16624−16631.
22. Xu, Y., and Beckett, D. (1994) *Biochemistry 33*, 7354−7360
23. Prakash, O., and Eisenberg, M. A. (1978) *J. Bacteriol. 134*, 1002−1012.
24. Buoncristiani, M. R., and Otsuka, A. J. (1988) *J. Biol. Chem. 263*, 1013−1016.
25. Wilson, T. J., Maroudas, P., Howlett, G. J., and Davidson, B. E. (1994) *J. Mol. Biol. 238*, 309−318.
26. Kar, S. R., Adams, A. C., Lebowitz, J., Taylor, K. B., and Hall, L. M. (1997) *Biochemistry 36*, 15343−15348.
27. Cheskis, B., and Freedman, L. P. (1996) *Biochemistry 35*, 3309−3318.
28. Zechel, C., Shen, X.-Q., Chen, J.-Y., Chen, Z.-P., Chambon, P., and Gronemeyer, H. (1994) *EMBO J. 13*, 1425−1433.
29. Green, S. M., Gittis, A. G., Meeker, A. K., and Lattman, E. E. (1995) *Nat. Struct. Biol. 2*, 746−751.
30. Metallo, S. J., and Schepartz, A. (1997) *Nat. Struct. Biol. 4*, 115−117.

BI991241Q